Electronic Supplementary Information (ESI)

Hydrophilic Ni_3S_2-MoN heterostructure on Ni foam (Ni_3S_2-MoN/NF) as an electrocatalyst for enhanced hydrogen evolution in alkaline media

Yeji Choi,[a] Jae Young Kim,[*b] Hyung-Kyu Lim[*a] and Duck Hyun Youn[*a]

[a] Department of Chemical Engineering, Department of Integrative Engineering for Hydrogen Safety, Kangwon National University, Chuncheon 24341, South Korea

[b] Korea Research Institute of Chemical Technology, Daejeon 34114, South Korea

*Corresponding authors

E-mail address: youndh@kangwon.ac.kr (D.H.Y.), hklim@kangwon.ac.kr (H.-K.L.), jaeykim@krict.re.kr (J.Y.K.)

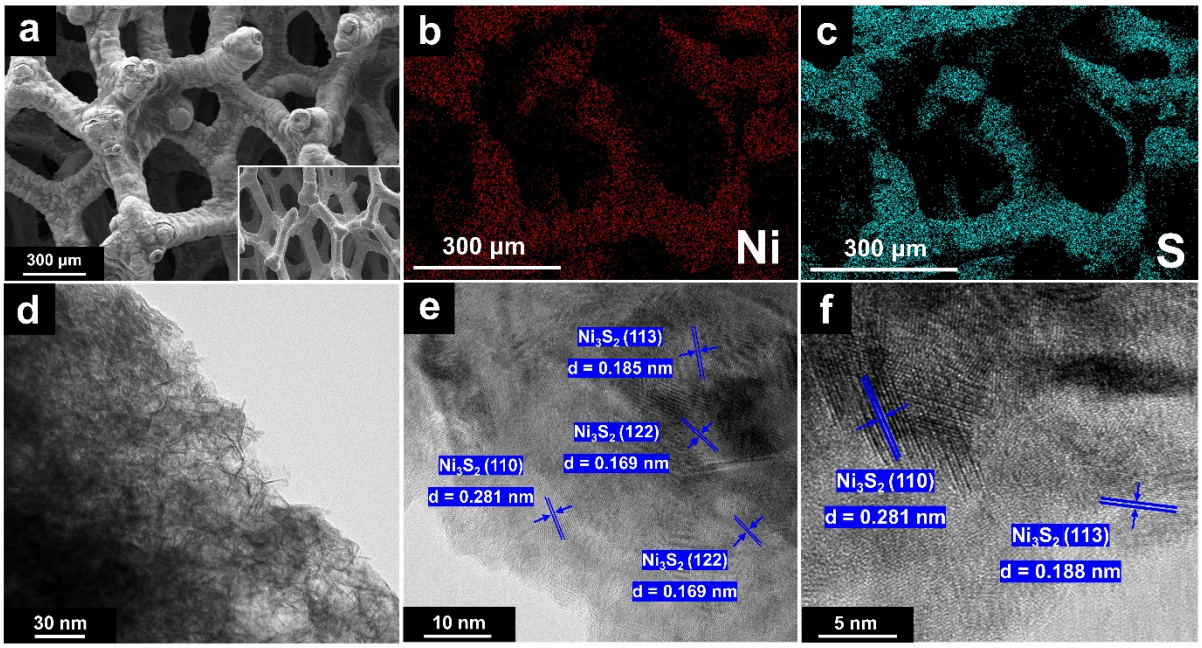

Fig. S1 a) SEM image of Ni_3S_2/NF (inset: SEM image of bare NF). EDS elemental mapping images of b) Ni and c) S in Ni_3S_2/NF. d) TEM and e, f) HRTEM images of Ni_3S_2/NF.

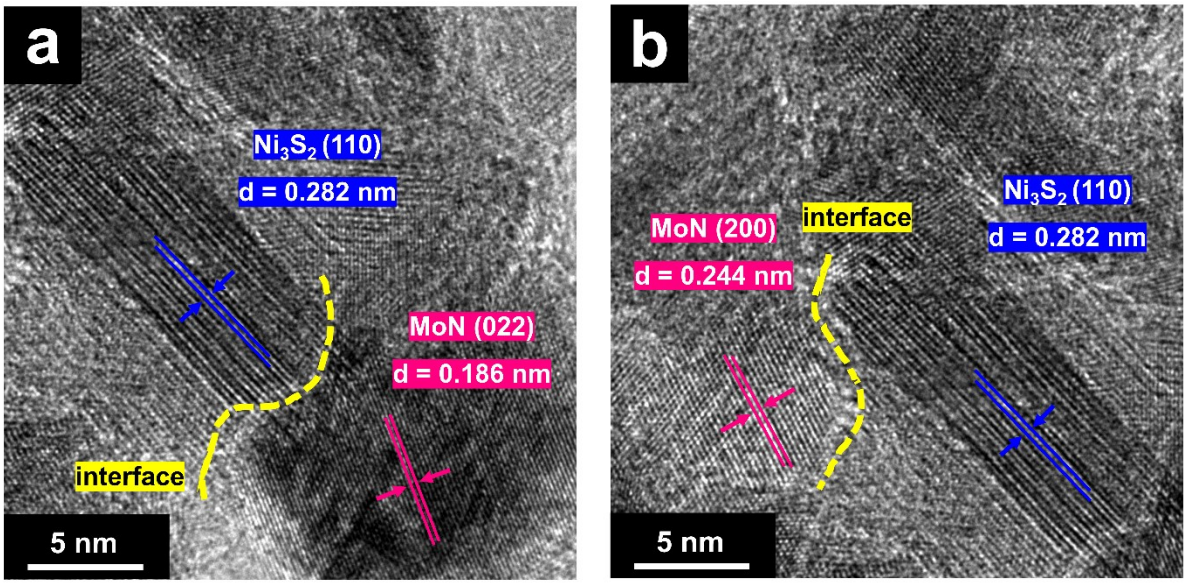

Fig. S2 a, b) HRTEM images of Ni_3S_2-MoN/NF.

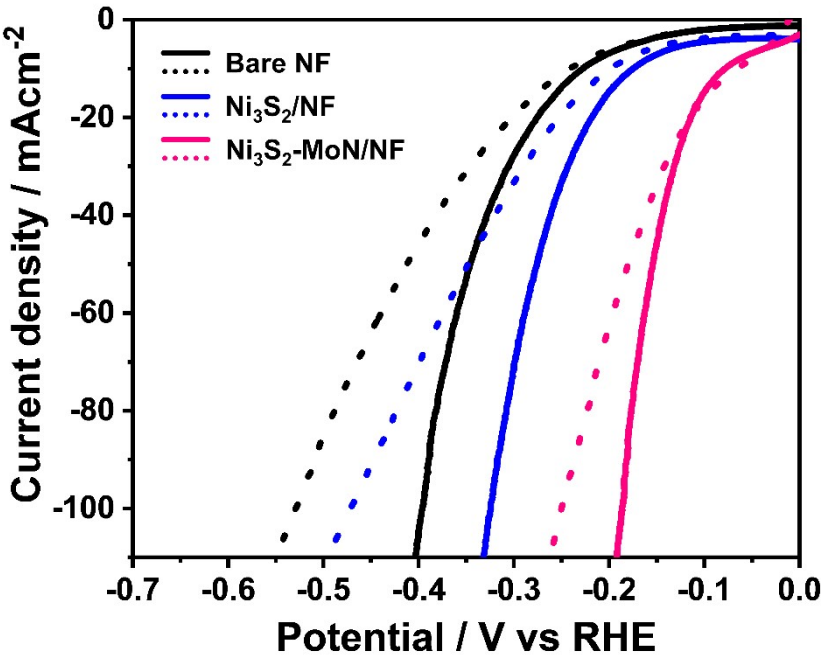

Fig. S3 Comparison of polarization curves with (solid line) and without (dotted line) iR compensation for Bare NF, Ni_3S_2/NF, and Ni_3S_2-MoN/NF in 1.0 M KOH.

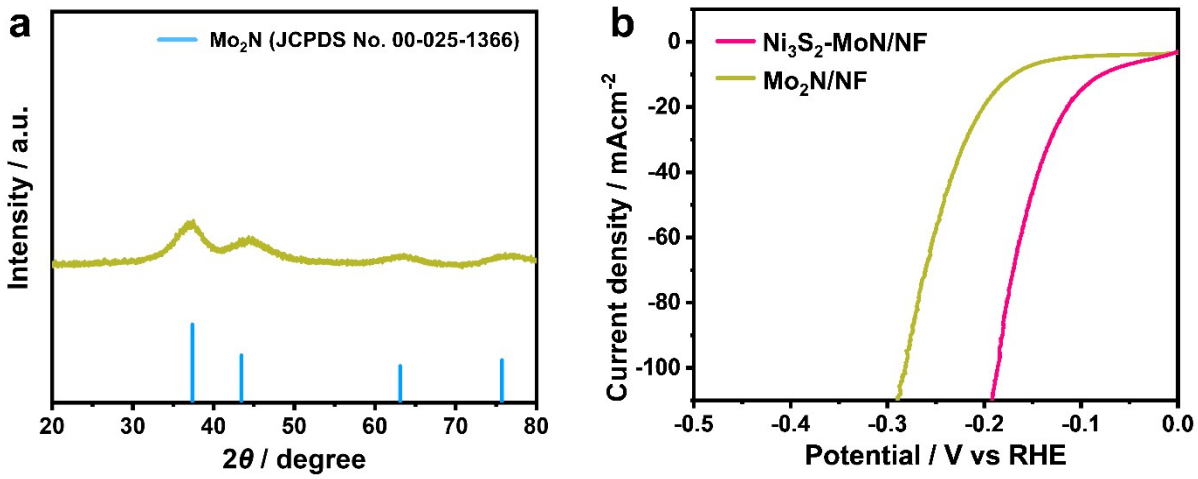

Fig. S4 a) XRD patterns of the prepared Mo_2N catalyst. b) Polarization curves of Mo_2N/NF and Ni_3S_2-MoN/NF in 1.0 M KOH.

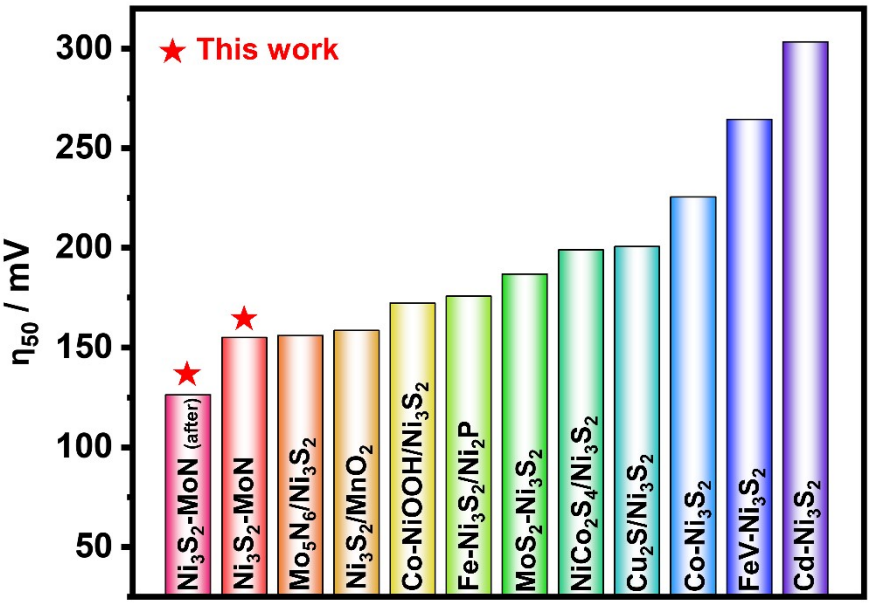

Fig. S5 Comparison of overpotentials at 50 $mAcm^{-2}$ (η_{50}) of Ni_3S_2-MoN/NF and reported Ni_3S_2-based catalysts. This graph was plotted based on Table S1.

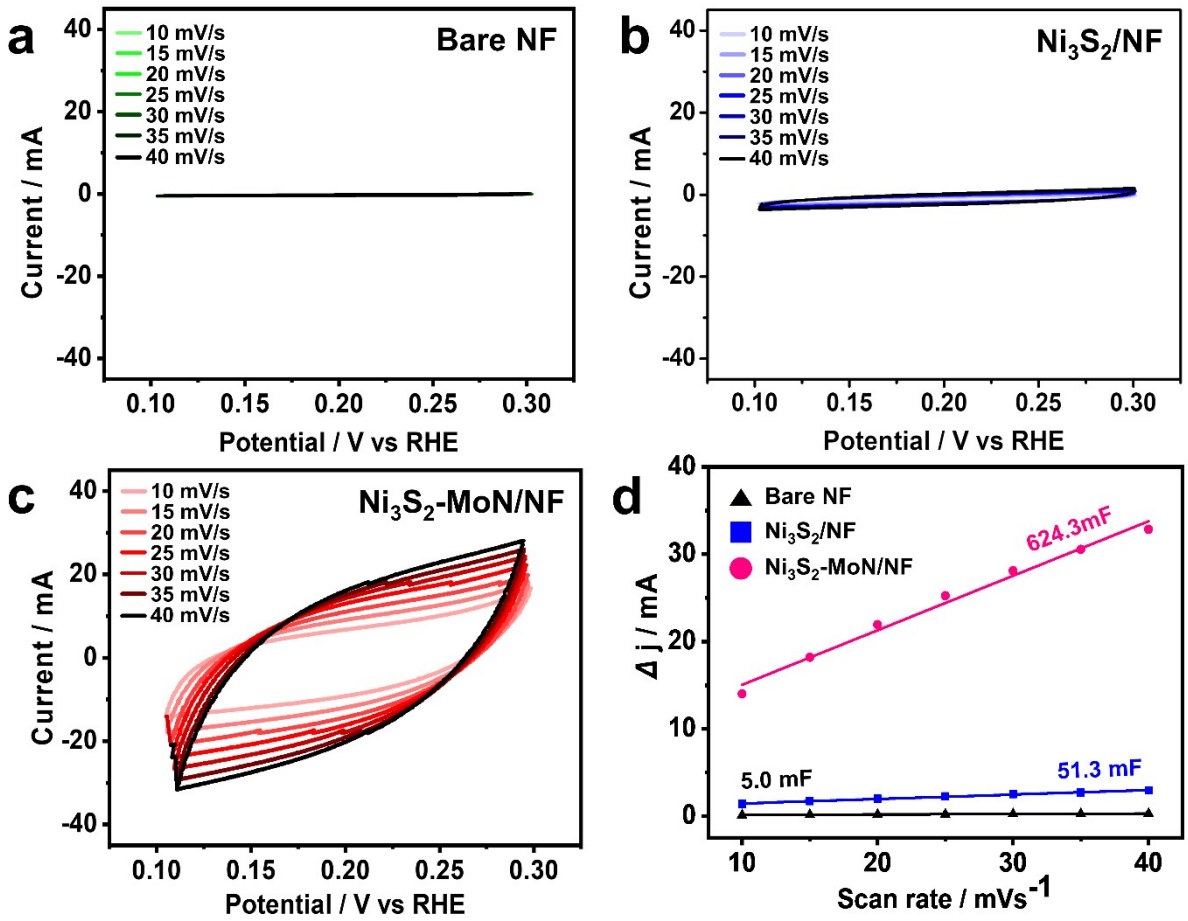

Fig. S6 Cyclic voltammograms in 1.0 M KOH for a) bare NF, b) Ni_3S_2/NF and c) Ni_3S_2-MoN/NF within a potential range of 0.1~0.3 V at different scan rates. d) C_{dl} values of Bare NF, Ni_3S_2/NF and Ni_3S_2-MoN/NF.

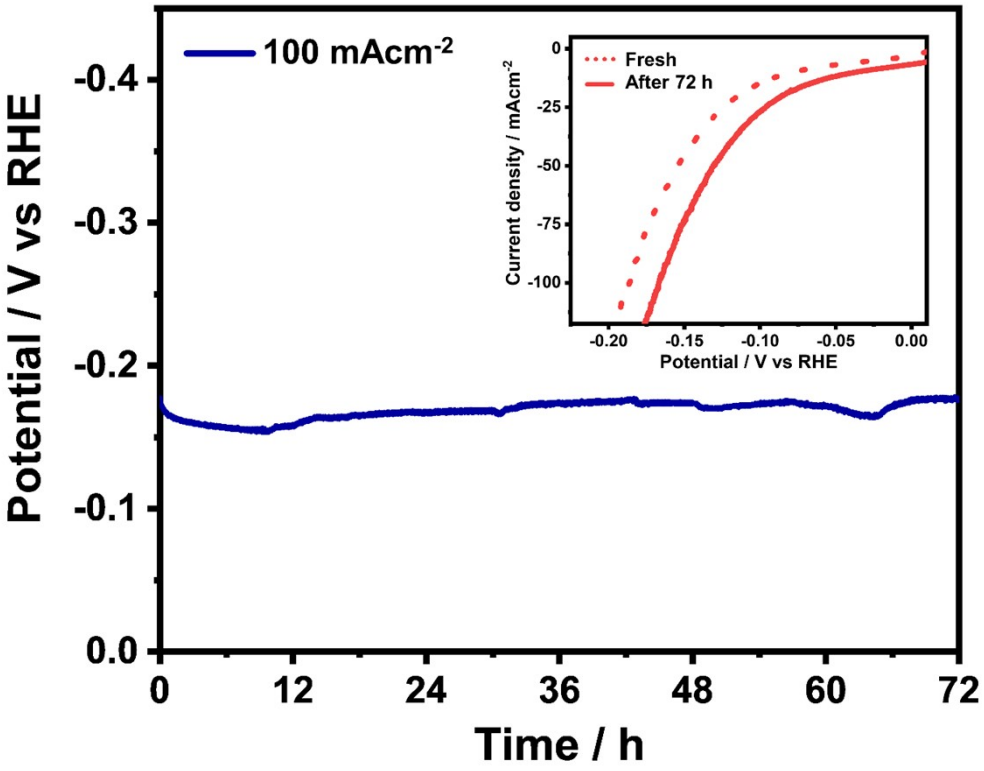

Fig. S7 Chronopotentiometry of Ni_3S_2-MoN/NF in 1.0 M KOH at 100 $mAcm^{-2}$ for 72 h. Inset denotes polarization curves of fresh and after sample.

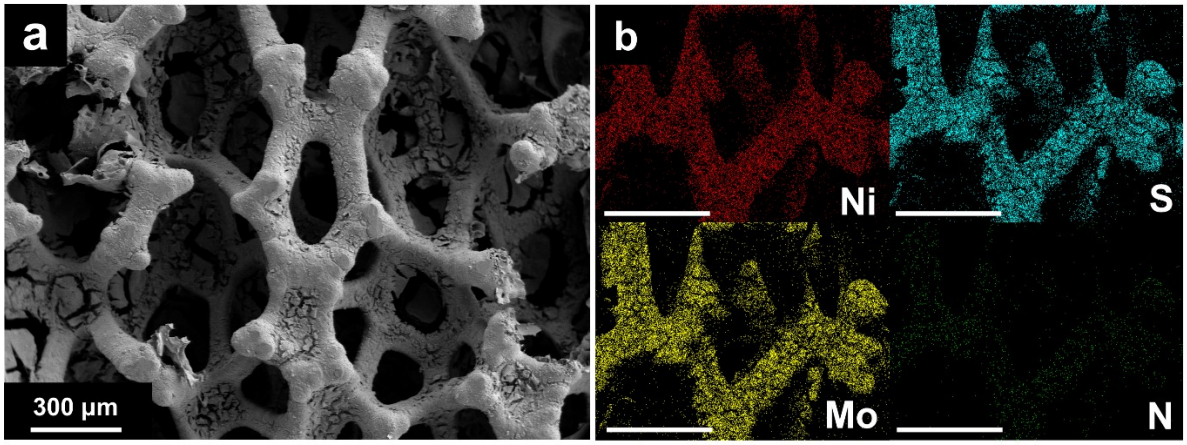

Fig. S8 a) SEM image of Ni_3S_2-MoN/NF after sample**.** b) EDS elemental mapping images of Ni, S, Mo, and N in Ni_3S_2-MoN/NF after sample**.**

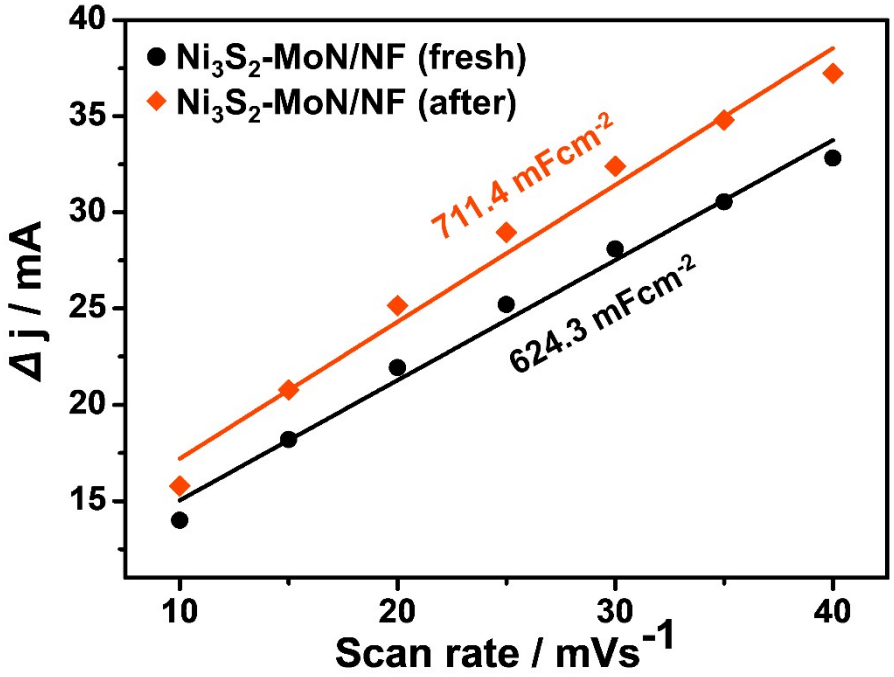

Fig. S9 C_{dl} values of Ni_3S_2-MoN/NF fresh and after sample.

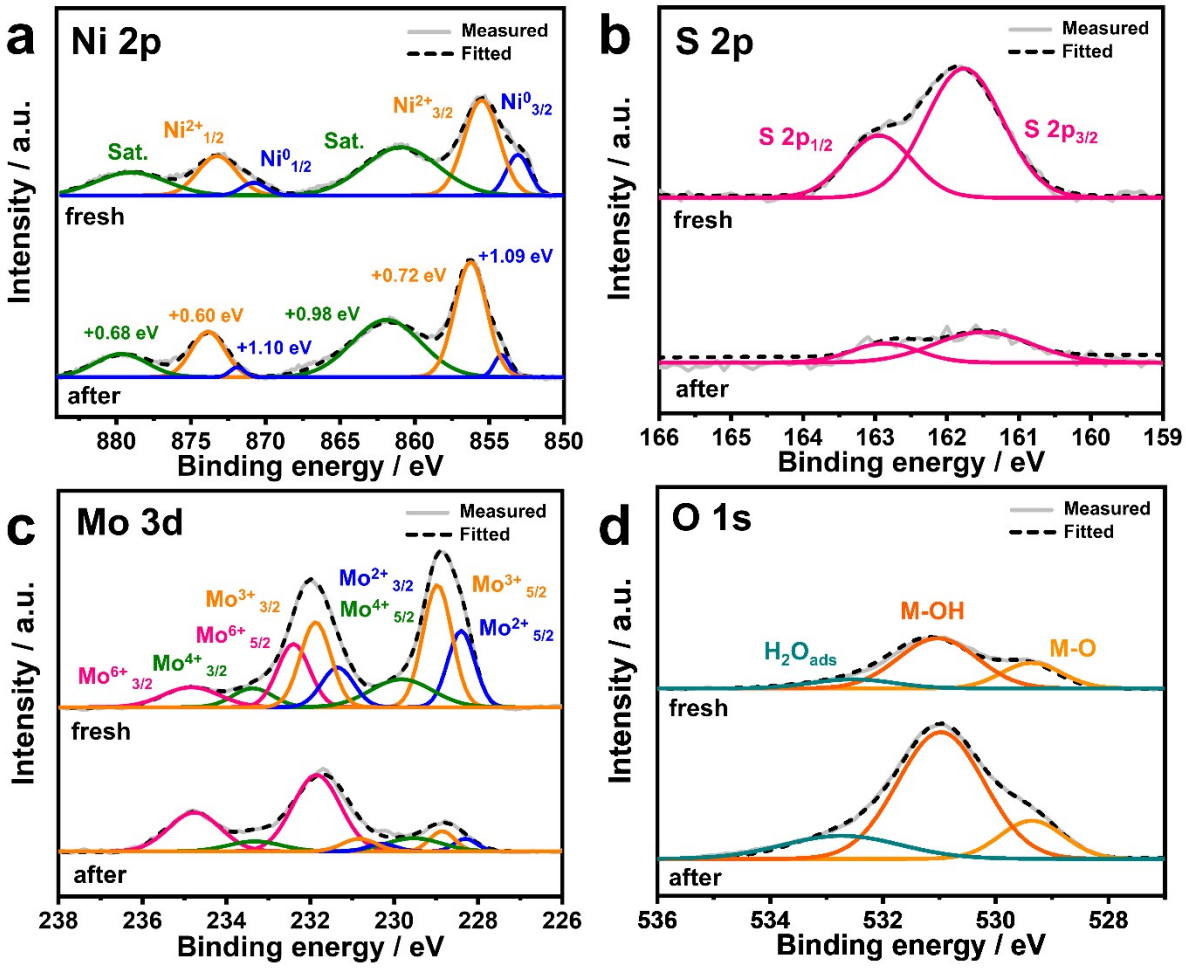

Fig. S10 Comparison of fresh and after sample (Ni_3S_2-MoN/NF) XPS spectra. a) Ni 2p, b) S 2p, c) Mo 3d, and d) O 1s

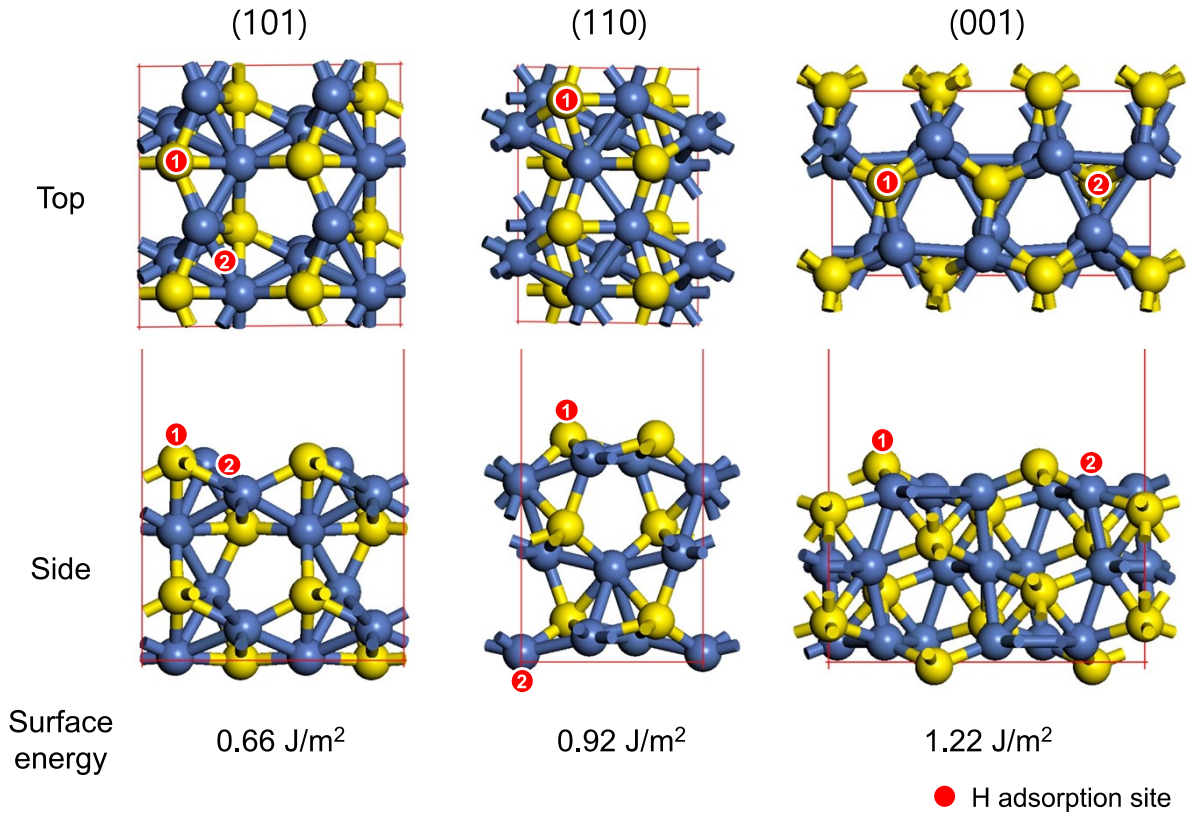

Fig. S11 Identification of potential hydrogen adsorption sites on different crystallographic surfaces of Ni_3S_2. The S and Ni binding sites are labeled as (1) and (2) on the top and side views of (101), (110), and (001) surfaces. These labeled sites correspond to the positions where hydrogen binding energies (HBE) were calculated in Fig. 7a.

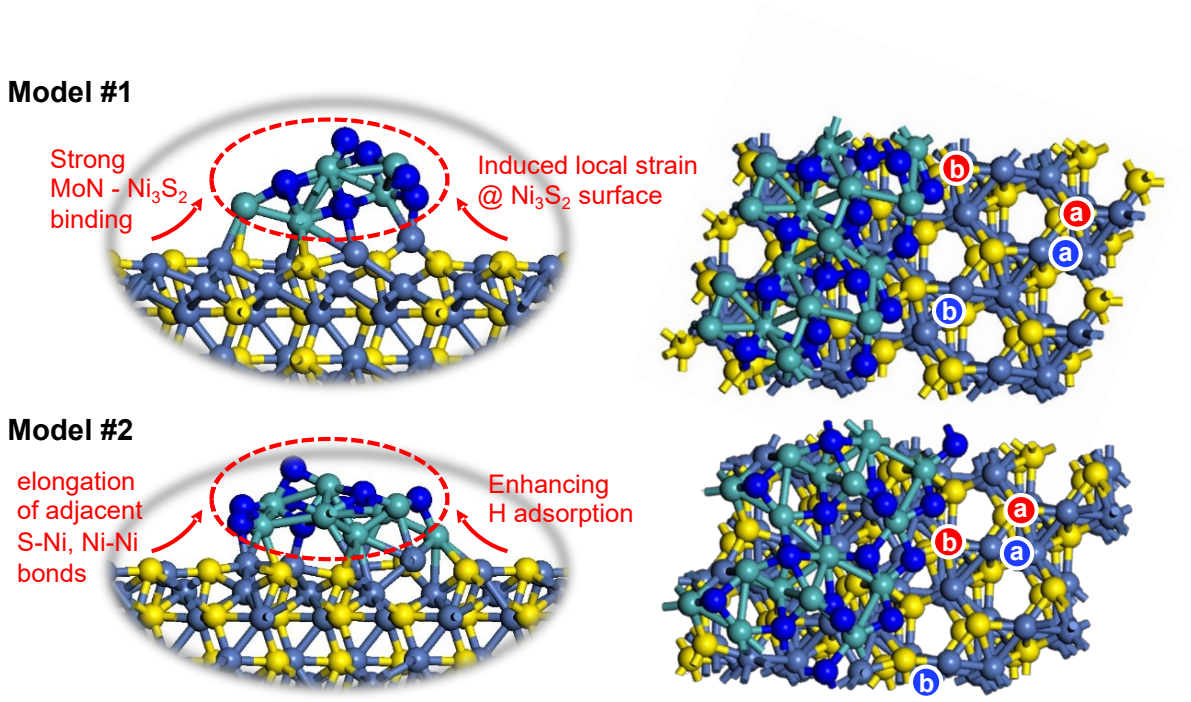

Fig. S12 Hydrogen binding sites at different Ni_3S_2-MoN junction structures. Red labels indicate S sites and blue labels indicate Ni sites. Sites marked as (a) are distal to MoN, while sites marked as (b) are adjacent to MoN.

Table S1. Comparison of Ni_3S_2-based HER catalysts in alkaline media (1.0 M KOH)

Catalyst	Substrate	η_{50} (mV)	η_{100} (mV)	Synthesis method	References
Ni_3S_2	NF	275.9	324.3	One step annealing	This work
Mo_2N	NF	242.4	281.7	One step annealing	This work
Ni_3S_2-MoN	NF	154.3	186.3	One step annealing	This work
Ni_3S_2-MoN (after)	NF	125.5	158.2	One step annealing	This work
Ni_3S_2/MnO_2	NF	157.7	198.9	Two step hydrothermal	[1]
Cu_2S/Ni_3S_2	NF	200.0	n/a	Two step hydrothermal	[2]
Mo_5N_6/Ni_3S_2	NF	155.2	313.0	Hydrothermal followed by annealing	[3]
$NiCo_2S_4/Ni_3S_2$	NF	198.3	n/a	Two step hydrothermal	[4]
Co-NiOOH/Ni_3S_2	NF	171.6	210.8	Hydrothermal followed by electrodeposition	[5]
MoS_2-Ni_3S_2	NF	186.2	214.7	Two step hydrothermal followed by annealing	[6]
Fe-Ni_3S_2/Ni_2P	NF	175.0	198.7	Two step hydrothermal followed by annealing	[7]
Cd-Ni_3S_2	NF	303.3	435.4	Two step hydrothermal	[8]
Co-Ni_3S_2	NF	225.0	n/a	Two step hydrothermal	[9]
FeV-Ni_3S_2	NF	264.6	309.1	Two step hydrothermal	[10]

* The data values in the table are estimated based on the referenced paper.

References

[1] Y. Xiong, L. Xu, C. Jin and Q. Sun, *Appl. Catal. B*, 2019, **254**, 329-338.

[2] Y. Peng and H. He, *RSC Adv.*, 2021, **11**, 39493-39502.

[3] B. Fang, J. Jin, Y. Li, H. Dang, M. Shao, L. Zhao, N. Yin and W. Wang, *Small*, 2024, **20**, 2310825.

[4] X. Xu, Q. Liu, W. Zhong, L. Zhang, Y. Lu and Y. Du, *Int. J. Hydrog. Energy*, 2021, **46**, 39226-39235.

[5] Z. Wu, Y. Feng, Z. Qin, X. Han, X. Zheng, Y. Deng and W. Hu, *Small*, 2022, **18**, 2106904.

[6] H. Liu, D. Ouyang, Q. Zhou and C. Feng, *J. Alloys Compd.,* 2022, **920**, 165243.

[7] X. Wang, X. Yu, J. Bai, G. Yuan, P. He, Y. Zhu, S. Wu, F. Qin and L. Ren, *Electrochim. Acta*, 2023, **458**, 142534.

[8] H. Yan, R. Deng, S. Zhang, H. Yao, J. Duan, H. Bai, Y. Li, R. Liu, K. Shi and S. Ma, *J. Alloys Compd.*, 2023, **954**, 170072.

[9] K. Sun, F. Qiao, J. Yang, H. Li, Y. Cui and P. F. Liu, *Int. J. Hydrog. Energy*, 2022, **47**, 27986-27995.

[10] P. Krishnamurthy, A. Kumar, S. A. Alqarni, S. Silambarasan and T. Maiyalagan, *Surf. Interfaces*, 2024, **44**, 103694.